

Lasers in Manufacturing Conference 2019

## Heat treatment of SLM-LMD hybrid components

Eckart Uhlmann<sup>a,b</sup>, Jan Düchting<sup>a\*</sup>, Torsten Petrat<sup>b</sup>, Benjamin Graf<sup>b</sup>,  
Michael Rethmeier<sup>a,b,c</sup>

<sup>a</sup>Technische Universität Berlin, Institute of Machine Tools and Factory Management, Pascalstraße 8-9, 10587 Berlin, Germany

<sup>b</sup>Fraunhofer Institute for Production Systems and Design Technology, Pascalstraße 8-9, 10587 Berlin, Germany

<sup>c</sup>Federal Institute for Materials Research and Testing, Unter den Eichen 87, 12205 Berlin, Germany

---

### Abstract

Additive manufacturing is no longer just used for the production of prototypes but already found its way into the industrial production. However, the fabrication of massive metallic parts with high geometrical complexity is still too time-consuming to be economically viable. The combination of the powder bed-based selective laser melting process (SLM), known for its geometrical freedom and accuracy, and the nozzle-based laser metal deposition process (LMD), known for its high build-up rates, has great potential to reduce the process duration. For the industrial application of the SLM-LMD hybrid process chain it is necessary to investigate the interaction of the processes and its effect on the material properties to guarantee part quality and prevent component failure. Therefore, hybrid components are manufactured and examined before and after the heat treatment regarding the microstructure and the hardness in the SLM-LMD transition zone. The experiments are conducted using the nickel-based alloy Inconel 718.

Keywords: Additive Manufacturing; Selective Laser Melting; Laser Metal Deposition; Inconel 718; hybrid components

---

### 1. Introduction

Additive manufacturing processes have become very popular in the recent past. The new geometrical freedom of design has great potential to overcome limitations of conventional manufacturing processes and therefore it becomes possible to focus on the component function. The great potential and the continuous

---

\* Corresponding author. Tel.: +49 (0) 30 / 314 23624; fax: +49 (0) 30 / 314 25895.  
E-mail address: jan.duechting@iwf.tu-berlin.de.

improvement of the processes led to an increased usage in the industrial environment, as indicated in the annual Wohlers Report, Caffrey et al., 2018. However, manufacturing costs and process durations are still drawbacks of prominent additive manufacturing processes, like Selective Laser Melting (SLM). Especially the production of massive parts requires long production times, due to the small laser spot diameter. In the recent years, many efforts were made to reduce the SLM process duration and therefore the manufacturing costs. One approach is the usage of a multi beam system, Buchbinder et al. 2011, as well as the usage of a higher laser power to melt multiple layers at the same time, Bremen et al., 2011. Another approach is the hybrid additive-additive manufacturing by using the fast laser metal deposition (LMD) process for massive regions of the component and the SLM process for regions, which require a high resolution. The LMD process features a larger laser beam spot and therefore the build-up rate is comparatively higher whereas the resolution is not as high as with the SLM process. This hybrid approach was demonstrated in previous experiments at the Fraunhofer IPK, Graf et al., 2015, by printing a turbine blade, where the upper part with its grid structure and cooling channels was produced with SLM and the massive fir-tree root was added in a subsequent LMD process. Thereby the production time was reduced from 13.85 h to 5.35 h. Besides the time-saving aspect, it was demonstrated that this approach can also be used to repair SLM components with LMD, Petrat et al., 2016, as well as to embed electronics in SLM structures, Petrat et al., 2018. The combination of the SLM and LMD process in one hybrid additive process chain has the potential to benefit from the different advantages of each of the processes, as indicated in table 1. However, the mechanical properties in the SLM and the LMD region are different and therefore the fatigue behaviour of the hybrid component differs as well, especially in the transition zone, as shown by Petrat et al. for Inconel 718, 2016, and Liu et al. for Ti6Al4, 2016. The transition zone is the heat-affected zone (HAZ) in the SLM part and is a result of the subsequent LMD heat input. Therefore, this work focusses on how the transition zone, as well as the SLM and LMD region, react to a subsequent heat treatment and if the heat treatment leads to uniform mechanical properties of the hybrid compound.

Table 1. Comparison of the SLM and LMD process

Process	Typical laser spot diameter & power	Part dimensions	Structural complexity	Substrate	Material flexibility
Selective Laser Melting	100 $\mu\text{m}$ , 300 W	Small to medium (limited by process chamber)	High (e.g. lattice structures)	Flat surfaces	Same powder for whole process
Laser Metal Deposition	1 mm, 1 kW	Medium to large (limited by machine working area)	Limited (e.g. walls)	Freeform surfaces	In-process change of powder

## 2. Experimental methods

To validate the influence of heat treatment on hybrid SLM-LMD components, massive SLM parts are used as a substrate for the subsequent LMD process. The hybrid components are investigated in the as-build condition and after heat-treated condition.

### 2.1. The additive manufacturing processes SLM and LMD

The production sequence of the SLM technology essentially consists of three repetitive steps. First, a thin layer of metal powder is placed on a platform with a wiper, as illustrated in figure 1a. In the second step, a

focused laser beam melts the powder layer selectively and in the third step the platform is lowered by the layer thickness to begin once again with the powder deposition. These steps are repeated until the part is finished.

In the LMD process, the material feed is realized by a powder nozzle, as pictured in figure 1b. The nozzle guides the laser beam as well as the shielding gas, which prevents oxidation, and the carrier gas for the transportation of the powder particles. The laser beam creates a molten pool on the base material. The powder particles are injected in the melt pool and therefore single weld beads are formed after solidification. The deposition of layers and volumes are realized by placing multiple weld beads next to each other.

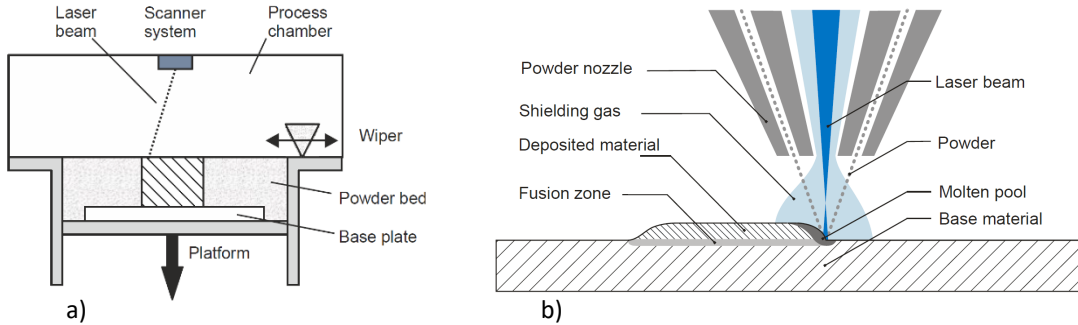


Fig. 1. Schematic illustration of the a) SLM process; b) LMD process

## 2.2. Fabrication of the SLM-LMD specimens

The Inconel 718 SLM parts are manufactured with the SLM machine *SLM 250HL* from SLM SOLUTIONS GMBH, Lübeck, Germany, which contains a YLR 400W Yb:Yag fiber laser from IPG PHOTONICS CORPORATION, Oxford, USA. The SLM process is conducted with the standard parameters for Inconel 718 from SLM SOLUTIONS GMBH, Lübeck, Germany, which are represented by the volume parameters in table 2. The used Inconel 718 powder exhibits a grain size distribution of 20  $\mu\text{m}$  to 63  $\mu\text{m}$  and is deposited with a layer thickness of 50  $\mu\text{m}$ . For the laser exposure a zigzag build-up strategy is chosen, where the scan vectors rotate by 33° with each layer. To prevent oxidation during the build-up, the build chamber is filled with Argon 5.0. For the SLM part geometry, a 20 x 20 x 10 mm cuboidal block is chosen. After manufacturing, the top layer is remelted with the standard upskin parameters, which are given in table 2, to obtain a smooth upskin surface. After the removal of the part from the substrate, the LMD deposition of Inconel 718 on the SLM upskin surface is realized.

Table 2. SLM and LMD process parameters for Inconel 718

Standard parameters for Inconel 718	Laser Power [W]	Velocity [mm/s]	Laser spot diameter [mm]	Hatch distance [mm]
SLM Volume	275	760	0.18	0.12
SLM Upskin	300	400	0.18	0.18
LPA	750	12.5	1.0	1.22

The LMD experiments are conducted with the machine *TruLaser Cell 7020*, manufactured by TRUMPF GMBH + Co. KG, Ditzingen, Germany. The machine contains a *TruDisk* 2.0 kW Yb:Yag laser and coaxial powder nozzle, which is orientated perpendicular to the SLM upskin surface. The used powder has a grain distribution of 45  $\mu\text{m}$  to 90  $\mu\text{m}$  and was carried in Helium 5.0. With a fixed gas flow of 4 l/min, the powder mass flow was adjusted to 5.2 g/min. The used process parameters for good mechanical properties are derived from previous experiments and pictured in table 2. The resulting LMD track has a width of 1.85 mm and a track height of approximately 0.5 mm. In each layer the rectangular contour track is deposited first and then a zigzag build-up strategy is applied for the hatch, which is rotated by 90° in subsequent layers. The starting point of the contour track also varies in subsequent layers to prevent accumulating elevations. To avoid oxidation of the deposited Inconel 718, Argon 5.0 is used as shielding gas.

For the analysis of the transition zone, ten layers are deposited by LMD onto the SLM substrates. Additionally, the remelted depth of the SLM part due to the LMD surface remelting is investigated by coating only the half of the SLM surface with one layer. For the comparison of the SLM and LMD process duration, several 20 x 20 x 50 mm cuboids were manufactured.

### 2.3. Heat treatment and analysis

To equalize the mechanical properties of the Inconel 718 in the SLM and LMD section of the part, a standard heat treatment according to VDI 3405 is conducted, VDI standard, 2017. The heat treatment is conducted in the *LH 60/13* chamber furnace from NABERTHERM, Lilienthal, Germany. The initial step is a solution heat treatment with a temperature of  $T_1 = 980^\circ\text{C}$  for one hour. After air cooling to room temperature, the furnace is heated up again for a two-step artificial aging. The first step lasts 8 hours at  $T_2 = 720^\circ\text{C}$  and subsequent to a furnace cooling with a cooling rate of 4 K/min the second step follows with  $T_3 = 620^\circ\text{C}$  for 10 hours. The heat treatment process ends with an air cooling to room temperature and the removal of the specimens for the successive analysis.

For the analysis of the microstructure by means of optical microscopy, the heat-treated specimens as well as the specimens in the as-built condition are cut perpendicular to the build direction. The metallographic preparations start with inserting the specimens in an epoxy resin, followed by grinding and polishing with diamond suspension as well as a final treatment with hydrochloric acid and hydrogen peroxide at a ratio of 4 to 1. The prepared specimens are analyzed using the digital microscope *BX51* from the OLYMPUS CORPORATION, Tokyo, Japan. Finally, the Vickers hardness of the specimens is measured in the SLM, LMD and transition zone with the microhardness measuring system *H100VP* from HELMUT FISCHER GMBH, Sindelfingen, Germany. In total, 19 measurements for each specimen are conducted to provide an insight into the hardness distribution in the different areas.

## 3. Results and discussion

### 3.1. SLM and LMD build-up rate

To compare the build-up rates, the process differences must be taken into consideration. For instance, the build part height is important, because in the SLM process the process duration is composed of the time for melting the powder with the laser beam and the time to deposit a new powder layer with the wiper. The additional time for coating is taken into account by calculating the needed time to deposit one layer and

determining the additional duration for 200 layers, which is equivalent to 1 cm in height. The LMD process is not powder bed-based and therefore no additional time for powder deposition is needed. In table 3 the mean values for the build-up rate with standard parameters are given by taking various experiments into account, manufacturing massive 20 x 20 x 50 mm cuboids as test specimens for tensile testing. Neglecting the time for the coating, LMD is more than twice as fast as the SLM process. Taking the coating duration into account, additional 52 minutes can be saved for every centimeter in height if the massive part is printed by LMD instead of SLM. Exemplarily, this adds up to a production time saving of 17.7 hours for a substitution of the SLM process by the LMD process, if applying the build-up rates on a SLM batch with 320 cm<sup>3</sup> build volume and a build height of 5 cm, as pictured in table 3. Consequently, the production time is reduced by 62 %.

Table 3. Built-up rates of SLM and LMD for massive parts

	Built-up rate	Additional production time	Duration for batch (16 cuboids with 20 x 20 x 50 mm <sup>3</sup> )
SLM without coating	13.2 cm <sup>3</sup> /h	-	24.24 h
SLM coating duration (per height)	-	0.87 h/cm	4.35 h
LMD	28.5 cm <sup>3</sup> /h	-	10.88 h

### 3.2. LMD remelting depth

In figure 2 an unfinished LMD layer on a SLM substrate is shown. The consolidation and the resulting microstructure of the material is different for the SLM and LMD process and therefore the LMD remelting depth  $r$  is determined after etching the specimen. For the measurement of the LMD remelting depth  $r$ , the level of the unmelted, even SLM surface, pictured as a white line in figure 2.

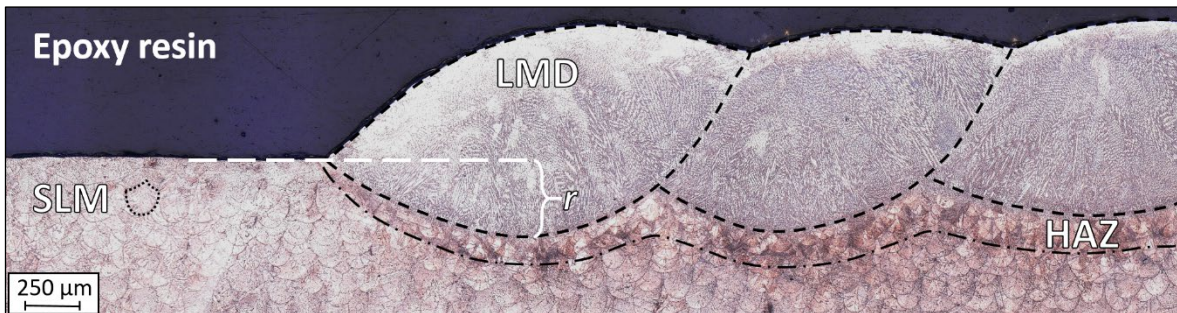


Fig. 2. Remelting depth  $r$  in as-built Inconel 718 SLM-LMD specimen with outlined melt pool boundaries and heat-affected zone (HAZ)

The depth of every weld bead is measured perpendicular from this SLM surface level to the bottom of the LMD weld bead. The remelting depth in the SLM specimen is ranging from  $r_{\min} = 0.14$  mm in the first weld bead to approximately  $r_{\max} = 0.34$  mm in the last weld bead, which is pictured in figure 2. The remelting

depth  $r$  is increasing because the exposure with the laser radiation is heating up the SLM substrate and therefore less energy is needed to heat up the substrate before remelting.

### 3.3. Microstructure with and without heat treatment

In figure 3 two representative specimens are pictured, where in figure 3a the as-built condition and in figure 3b the heat-treated condition is pictured. In both cases a good metallurgical bonding is achieved. However, the SLM area can be distinguished from the LMD area because the resulting microstructure differs from each other.

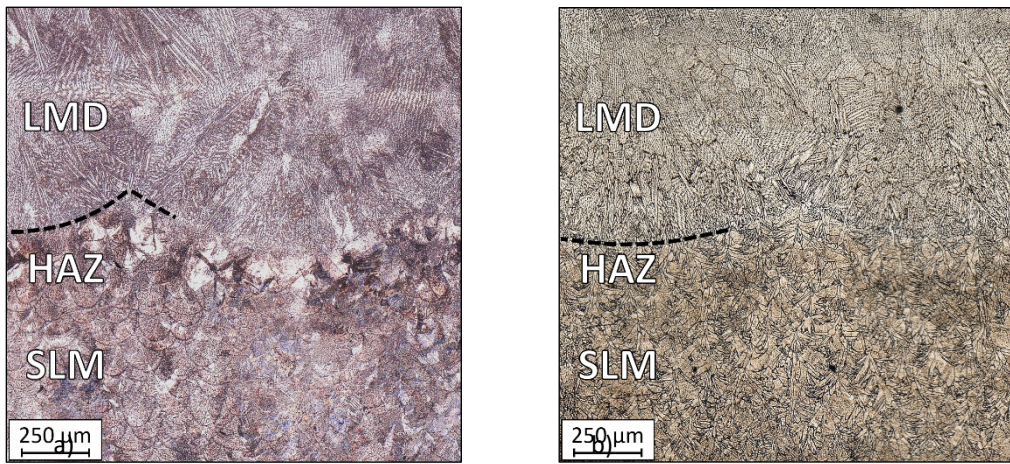


Fig. 3. SLM-LMD microstructure with indicated LMD melt pool boundary in the a) as-built condition; b) heat-treated condition

In the as-built condition the zigzag build-up strategies lead to the typical, layered cross-section with its alternating melt pool orientation. Corresponding to the used laser spot diameter, the LMD melt pool diameter is larger than the SLM melt pool. Additionally, the epitaxy contributes to the inhomogeneity of the microstructure because the direction of heat conduction drives crystal growth from the melt pool barrier to the center of the melt pool. The heat conduction also determines the size of the grains and the mechanical properties, because a higher cooling rate leads to larger grains and stiffer material, as pointed out by Poprawe, 2005. The finer grains in the SLM part are in accordance with the literature, due to the higher cooling rate in SLM processes, Poprawe, 2005.

The melt pool boundaries are visible due to the segregation of matrix elements during the consolidation and its different reaction to the etchant. Furthermore, the etched SLM part reveals a higher contrast in the transition zone next to the LMD area, which highlights the influence of the subsequent heat input by LMD on the SLM structure. Therefore, the transition zone is a heat-affected zone (HAZ). The elongation  $E_{HAZ}^{vis}(L)$  of the visible HAZ is expanding with the amount of deposited layers  $L$  due to the higher heat input by LMD. For one layer the HAZ elongation is  $E_{HAZ}^{vis}(1) = 154 \pm 20 \mu\text{m}$  and for ten layers it is  $E_{HAZ}^{vis}(10) = 279 \pm 17 \mu\text{m}$ .

After heat treatment, the distribution of elements is homogenized and therefore the SLM melt pool barriers, the build-up strategy as well as the HAZ are not visible and instead, a homogeneous and fine microstructure in the SLM and LMD part is achieved. Nevertheless, the SLM area is still clearly separated from the LMD area. The epitaxy and the resulting grain boundaries as well as the color after etching in each area differ from each other. This difference in microstructure can be explained by the influence of the initial microstructure. Since the atmosphere during heat treatment does not reach the liquidus temperature of Inconel 718, the crystals are not growing from the liquid phase but from unmelted seed crystals, which act as starting points for crystal growth and therefore affect the crystallographic orientation.

Furthermore, some LMD melt pool boundaries are still apparent, although they diminished in contrast. A possible explanation for the appearance of the LMD melt pool boundaries after the heat treatment is the lower cooling rate during the LMD process, which leads to a prolonged consolidation and therefore to a higher accumulation of segregated elements. These segregations are not fully dissolved during the solution heat treatment.

### 3.4. Microhardness before and after heat treatment

In figure 4a the method for the hardness measurement is exemplarily illustrated. The measured points are aligned in the vertical direction with a distance of 50  $\mu\text{m}$  between the measurement points, covering the SLM, HAZ and LMD area. The coordinate origin  $d_M = 0 \mu\text{m}$  is set to the lower end of the LMD area and aligned with the building direction, leading to positive measurement distances  $d_M$  in the LMD area. The corresponding distribution of the Vickers hardness as a function of the measuring distance  $d_M$  is pictured in figure 4b.

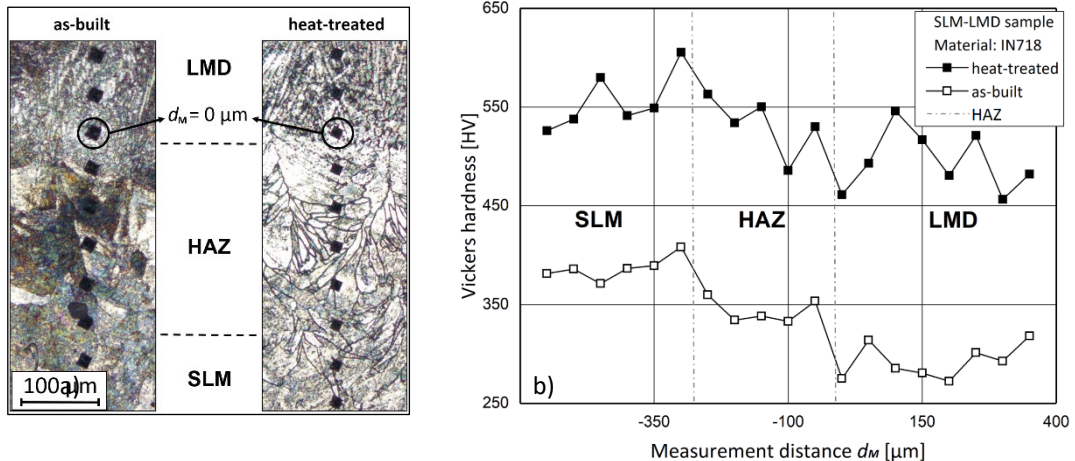


Fig. 4. Comparison of the hardness in the as-built and heat-treated condition. a) Illustration of measurement; b) Hardness distribution

In the as-built condition the range of the hardness values are consistent with the literature, VDI 3405 standard, 2017. In accordance to the finer grains in the SLM area, the hardness exceeds the LMD hardness. The reheating of the HAZ during the LMD process lowers the initial high SLM hardness and therefore the hardness values in the HAZ are located between the high SLM hardness and the low LMD hardness. In total, five measure points can be attributed to the HAZ and therefore the measurable elongation of the HAZ is

about  $E_{HAZ}^{hard} = 250 \mu m$ , which confirms the visual, metallurgical determination with an elongation of  $E_{HAZ}^{vis} = 279 \pm 17 \mu m$ .

In the heat-treated condition, the values indicate a higher hardness than the reported literature values according to VDI 3405 standard, 2017. The hardness in the SLM area is still higher than the hardness in the LMD region, but the mean values are similar with a small deviation of  $\Delta = 62 \text{ HV}$ , as illustrated in table 4.

Table 4. Mean values for the Vickers hardness in the different areas

Vickers Hardness	As-built condition	Heat-treated condition
SLM area $H_{SLM}$ [HV]	$387 \pm 12$	$557 \pm 30$
HAZ area $H_{HAZ}$ [HV]	$344 \pm 12$	$533 \pm 29$
LMD area $H_{LMD}$ [HV]	$292 \pm 17$	$495 \pm 31$
SLM-LMD deviation $\Delta = H_{SLM} - H_{LMD}$ [HV]	95	62

#### 4. Conclusion and outlook

The investigation shows that the combination of the SLM and LMD processes in a process chain can save a significant amount of production time, if massive parts of complex parts are fabricated by LMD instead of continuing with the SLM process. For a test batch, the production time is reduced by 62 %. Even if the additional time to change the manufacturing process is taken into consideration, the productivity increases using the hybrid process chain.

Moreover it is demonstrated, that a subsequent heat treatment enhances the uniformity of hybrid Inconel 718 SLM-LMD components. However, the measured hardness distribution indicates that even after heat treatment the hardness of the SLM part remains higher than the hardness of the LMD part. Additionally, the resulting microstructure after the heat treatment differs for the SLM and LMD part, which indicates an influence of the initial microstructure. Moreover, it was demonstrated that the LMD remelting depth is  $r = 0.34 \text{ mm}$  and the heat-affected zone due to the remelting reaches about  $280 \mu m$  into the SLM part after the deposition of ten LMD layers.

Further experiments are planned concerning the heat treatment and the uniformity of the hybrid component. For example, an extended duration of the solution heat treatment could lead to a higher uniformity of the mechanical properties, because the dissolution of segregations and seed crystals is promoted. To gain more insight into the mechanical properties and the fatigue behavior, tensile tests will be conducted. Moreover, the formation and elongation of the heat-affected transition zone will be further investigated.

## Acknowledgements

This paper is based on results acquired in the project Uh 100/251-1 or RE 1648/10-1, which is kindly supported by the Deutsche Forschungsgemeinschaft (DFG).

## References

- Caffrey, T., Wohlers, T., 2018. Wohlers Report 2018. Additive Manufacturing and 3D Printing State of the Industry.
- Buchbinder, D., Schleifenbaum, H., Heidrich, S., Meiners, W., Bültmann, J., 2011. "High Power Selective Laser Melting (HP SLM) of Aluminium Parts", *Phys. Procedia*, vol. 12, pp. 271-278.
- Bremen, S., Buchbinder, D., Meiners, W., Wissenbach, K., 2011. "Mit Selective Laser Melting auf dem Weg zur Serienproduktion?", *Laser Tech. J.*, vol 8, no. 6, pp. 271-278.
- Graf, B., Schuch, M., Kersting, R., Gumenyuk, A., Rethmeier, M., 2015. "Additive Process Chain using Selective Laser Melting and Laser Metal Deposition", *Laser in Manufacturing Conference*.
- Petrat, T., Graf, B., Gumenyuk, A., Rethmeier, M., 2016. "Laser metal deposition as repair technology for a gas turbine burner made of Inconel 718", *Physics Procedia*, vol. 83, pp. 761-768.
- Petrat, T., Kersting, R., Graf, B., Rethmeier, M., 2018. "Embedding electronics into additive manufactured components using laser metal deposition and selective laser melting", *Procedia CIRP*, vol. 74, pp. 168-171.
- Liu, Q., Wang, Y., Zheng, H., Tang, K., Ding, L., Li, H., Gong, S., 2016. "Microstructure and mechanical properties of LMD-SLM hybrid forming Ti6Al4V alloy", *Materials Science and Engineering A*, vol. 660, pp. 24-33.
- VDI standard 3405 Part 2.2, 2017. "Laser beam melting of metallic parts. Material data sheet nickel alloy material number 2.4668".
- Poprawe, R., 2005. "Lasertechnik für die Fertigung. Grundlagen, Perspektiven und Beispiele für den innovativen Ingenieur", Springer Verlag, pp. 177-180.